JOURNAL OF APPLIED ELECTROCHEMISTRY 24 (1994) 670–675

Study of pulsing flow in a trickle bed using the electrodiffusion technique

N. A. TSOCHATZIDIS, A. J. KARABELAS*

Chemical Process Engineering Research Institute and Department of Chemical Engineering, Aristotle University of Thessaloniki, Univ. Box 455, GR 540 06 Thessaloniki, Greece

Received 29 June 1993; revised 4 November 1993

An electrochemical technique is employed for measuring local, instantaneous liquid–solid mass transfer coefficients in downward cocurrent gas–liquid flow through a packed bed under pulsing flow conditions. The technique involves specially designed electrodes of the same dimensions as the packing material. Also microelectrodes on the surface of a particle are tested for flow diagnostics in the microscale. The feasibility of the method is examined. Interpretation of measurements from various electrodes provides information on the pattern of mass transfer and liquid distribution in the packing.

List of symbols

D diameter of the bed
D_L molecular diffusivity
d_p particle diameter
K_s liquid–solid mass transfer coefficient
r distance from the wall of the bed
Re_L liquid Reynolds number ($U_L d_p \rho_L / \mu_L$)
Sc Schmidt number ($\mu_L / \rho_L D_L$)
Sh Sherwood number ($K_s d_p / D_L$)
U_L liquid superficial velocity

Greek symbols
μ_L dynamic viscosity of the liquid
ρ_L density of the liquid
ϕ wetted fraction of the cathode

1. Introduction

Devices in which a gas and a liquid flow cocurrently downwards through a packed bed, simply called 'trickle beds', are extensively used in industrial processes for phase contacting and reaction. Among operations frequently carried out in trickle beds, are hydrodesulphurization, hydrocracking, catalytic hydrogenation and oxidation. Several reviews of this field are available in the literature; e.g. [1–4]. The theoretical and phenomenological aspects of trickle beds have been reviewed by Gianetto and Specchia [5].

Significant among the various flow regimes, observed in trickle beds, is 'pulsing flow' obtained under relatively high gas and liquid mass flow rates. The term pulsing flow refers to the alternating passage of liquid-rich and gas-rich two-phase flow down the packed column. This regime is attractive for many industrial applications because mass and heat transfer rates are enhanced, while axial dispersion is diminished [6, 7].

To predict the performance of trickle bed absorbers or reactors it is necessary to know the liquid distribution and the liquid–solid mass transfer rate. Three techniques are most frequently used for mass transfer measurements, based on the determination of the rate of: (i) dissolution of a soluble packing, (ii) gas adsorption and (iii) an electrochemical redox reaction. The latter offers the advantages of obtaining direct and instantaneous measurements and is thus very useful for measuring mass transfer fluctuations, especially under pulsing flow conditions [7]. The reported experimental work on this topic [7–9] provides useful information, but it is clearly insufficient to clarify basic aspects of pulsing flow and, in particular, mass transfer rates in the pulses as well as the temporal and spatial variation of mass transfer in the packing interstices.

Experimental results are reported here (using the well known electrodiffusion technique) on liquid–solid mass transfer in a trickle bed. Special electrodes are employed to measure local mass transfer rates. By comparing the results from single active particles (having the same dimensions as the packing material), placed in various radial locations, information about the radial liquid distribution in the bed can be extracted. Additionally, local measurements obtained with small circular electrodes, embedded onto the active particle surface, are helpful in improving understanding of flow characteristics in the bed interstices. A recent utilization of the electrochemical technique in a trickle bed, is reported by Latifi *et al.* [11] who analysed the signals of microelectrodes mounted in a non-conducting wall of a bed to determine flow regime transitions.

The particular objective of this work is to measure *local* liquid–solid mass transfer (and to draw conclu-

This paper was presented at the International Workshop on Electrodiffusion Diagnostics of Flows held in Dourdan, France, May 1993.

* Author for correspondence.

0021-891X 1994 Chapman & Hall

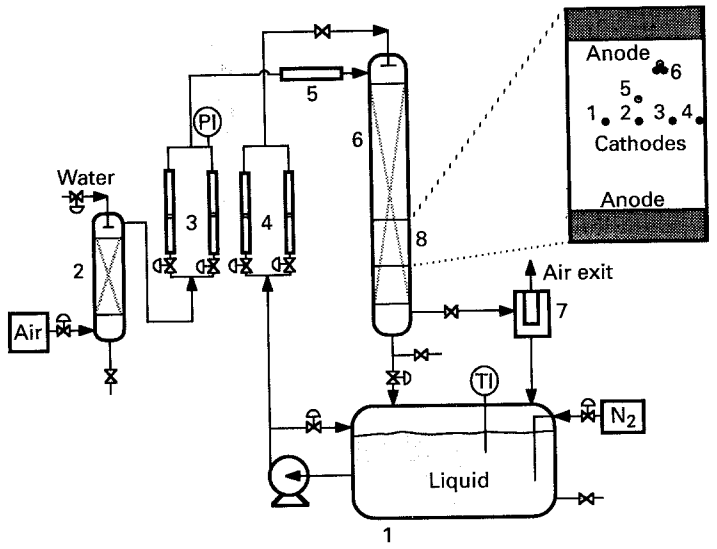

Fig. 1. Experimental setup and schematic diagram of the position of the electrodes. Key: (1) Liquid tank, (2) humidifier, (3) air rotameters, (4) liquid rotameters, (5) dampener, (6) packed column, (7) gas/liquid separator, and (8) test section.

sions regarding flow characteristics) in a length scale representative of the packing interstices, i.e. of order 10^{-1} to 10^{0} times the particle diameter. To test the techniques some initial experiments were performed in a full bed with liquid only.

2. Experimental setup and procedures

Experiments were carried out in a cylindrical column made of Plexiglas. The column i.d. was 14 cm and its length 124 cm. A schematic of the experimental system is shown in Fig. 1. The flow rates of air and liquid were measured by means of calibrated rotameters. Dry filtered air was saturated with water before entering the column, to avoid temperature gradients due to evaporation. To minimize air flow fluctuations a dampener was used. Liquid was collected in a tank and recirculated. Its temperature was continuously monitored and maintained at about 20° C. The liquid was sprayed uniformly onto the top of the packing through a perforated distributor and air was introduced by means of another perforated tubular section. The packing material was fairly uniform unpolished glass spheres of 6 mm diameter. The void fraction of the bed was 0.36. The packing material was supported, at the bottom of the column, by a rigid stainless steel screen.

The electrolytic solution was a mixture of 0.01 M potassium ferricyanide, 0.05 M potassium ferrocyanide and a large excess of 1 M sodium hydroxide as supporting electrolyte. The electrolytic solution in the liquid tank was kept in a nitrogen atmosphere to reduce the effects of dissolved oxygen. The solution was used for a short period of time (a few days) and then discarded. The measured density and viscosity of the solution at 20°C were $\rho_L = 1052\,\mathrm{kg\,m^{-3}}$ and $\mu_L = 1.38 \times 10^{-3}\,\mathrm{kg\,m^{-1}\,s^{-1}}$. The viscosity was corrected for small changes in temperature. The diffusivity of the ferricyanide was calculated from an equation given by Gordon *et al.* [11]. A detailed review of the limiting-current technique is presented by Selman and Tobias [12]. At high enough voltages the reaction rate is fast enough so that liquid–solid mass transfer is controlling. Under these conditions the limiting current is measured and the product ϕK_s is directly calculated. Here ϕ represents the fraction of the cathode area wetted by the electrolyte, and K_s is the liquid–solid mass transfer coefficient. In two phase systems only the product ϕK_s can be determined, since the actual effective active area is unknown. Instantaneous data of the product ϕK_s were obtained by measuring the limiting current to a cathode under diffusion controlling transport.

Various cathode types were employed (Fig. 1). To examine the radial dependence of the mass transfer coefficient four nickel spheres, of the same diameter as those of the packing, were placed along a diameter of the bed. Each was connected separately to the measuring circuit with a 0.5 mm insulated wire. The small reduction in the mass transfer area (resulting from the connection of the sphere with the wire) was taken into account in the calculations. Two thin nickel foils with large surface area (5 cm × 44 cm each) were used as the anode. The nickel foils were flush mounted to the column wall covering the entire circumference and located one upstream and the other downstream of the cathodes. This configuration was used to provide a better potential distribution in the solution and to reduce the ohmic potential drop between the electrodes [7]. The electrodes were installed at the lower part of the bed, relatively close to probes for other types of measurements [20]. The column height upstream of the electrodes (about 90 cm) is more than adequate for flow development [1], whereas their distance from the bottom (about 35 cm) is considered sufficient to avoid end effects.

Microelectrodes were prepared and installed in the following way (Fig. 2). A hole was drilled into a nickel sphere along a diameter. A nickel wire of 1 mm diameter sheathed in a thin PTFE tube, was fitted into the hole. The exposed end of the wire was polished to give a mirror-bright surface. By this procedure each microelectrode had the appearance of a circular nickel disc surrounded by an insulating ring. Jolls and Hanratty [15] and Karabelas *et al.* [17] used similar microelectrodes to study the details of the flow

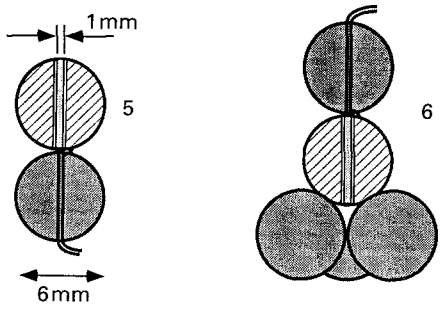

Fig. 2. A side view of microelectrode installation; electrodes 5 and 6.

around a particle in single phase flow through packed beds. Separate electrical connections of the microelectrode and of the rest of the nickel sphere were made, to activate them independently. One such sphere was placed at the centre of the column cross section with the microelectrode (electrode 5, Fig. 1) facing the flow.

To locate a microelectrode at a dense packing constriction, a pore was constructed using four spheres (1 nickel-active, 3 inert) of the same diameter as the packing material (Fig. 2). The centres of the four spheres formed a regular tetrahedron. The base of the tetrahedron (formed by the three inert spheres) was perpendicular to the column axis. Microelectrode 6 (Fig. 1) was facing the centre of the tetrahedron and the bottom of the bed. Thus the closest packing arrangement was formed, or the smallest three dimensional constriction.

The diffusion current was converted to voltage using precision resistances, amplified, digitized and stored in a computer. A separate circuit was employed for each cathode. A sampling rate of 100 Hz was considered sufficient and data were collected over a time period of 20.48 s. The column was always operated first under conditions of high liquid flow rates, to ensure complete wetting of the packing, and then the flow rates were set at the desired values.

3. Results and discussion

3.1. *Single phase flow*

In order to test the electrochemical system, initial runs were carried out with the bed full of liquid, i.e. in single phase flow. Only the spherical electrode placed at the centre of the bed cross section was used in these tests. Fig. 3 displays very good agreement between the new data and similar results from the literature. The correlation of Specchia *et al.* [13] was obtained from data taken by the technique of dissolution of benzoic acid cylinders. Hirose *et al.* [14] employed the dissolution as well as the electrodiffusion technique with 2.8 to 12.7 mm spheres as packing material. Jolls and Hanratty [15] and Karabelas *et al.* [16] used the same technique employed here (with random and regular packing of spheres, respectively) and various sizes of particles. An expression fitting the new data is also presented in Fig. 3.

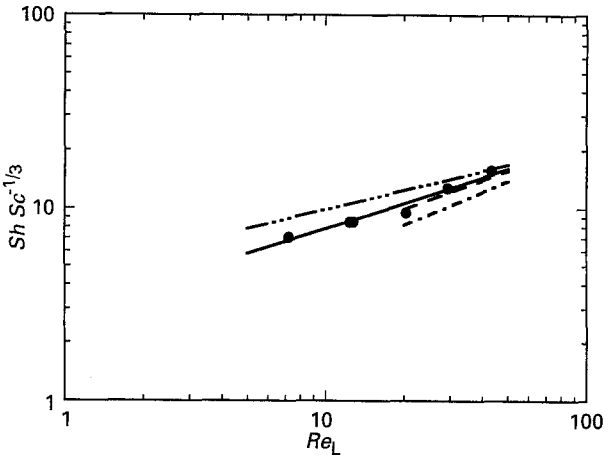

Fig. 3. Comparison between data for liquid filled bed and correlations from the literature. $ShSc^{-1/3} = 2.756Re_L^{0.45}$. Key: (——) Specchia *et al.* (1978), (– –) Hirose *et al.* (1976), (– · – · –) Jolls and Hanratty (1969), (– · · ·) Karabelas *et al.* (1971), (●) data of this work.

Some runs were carried out in the trickling flow regime without and with cocurrent gas flow, in the so-called gas continuous flow regime. Agreement of the new data with existing correlations is quite good.

3.2. *Pulsing flow in the microscale*

Knowledge of the gas and liquid flow characteristics in the length scale of particle radius are of great importance as they may be responsible for phenomena observed in the macroscale. Indeed, the constrictions of the bed porosity offer the greatest resistance to capillarity dominated displacement of one fluid by another and to viscous flow of two fluids moving together [6]. Furthermore, in reacting systems fluid stagnation, or poor mixing, may cause excessive localized heating and formation of hot spots which are a major problem in the operation of commercial tickle beds. On the basis of meagre data, it is considered that operation in the pulsing flow regime reduces such phenomena due to increased wetting of the packing, enhanced transport coefficients and improved uniformity of the flow [8]. A relevant question here is to what extent the fluctuations associated with pulsing flow (observed macroscopically) affect flow characteristics and transfer rates in the interstices.

A number of papers have appeared in the literature recently in which the microscale phenomena in a packed bed are investigated in order to describe and model the macroscale flow regimes [6, 18, 19]. To address the same problem circular microelectrodes were employed, flush mounted on the surface of a packing particle. Their arrangement is described in Section 2 (Fig. 2).

Simultaneously recorded signals from the two microelectrodes (5 and 6) and from the four spherical electrodes (1 to 4) placed along a bed diameter, are presented in Fig. 4. The regularity of fluctuations is due to the passage of pulses. The steep increase of the limiting current is apparently caused by the pas-

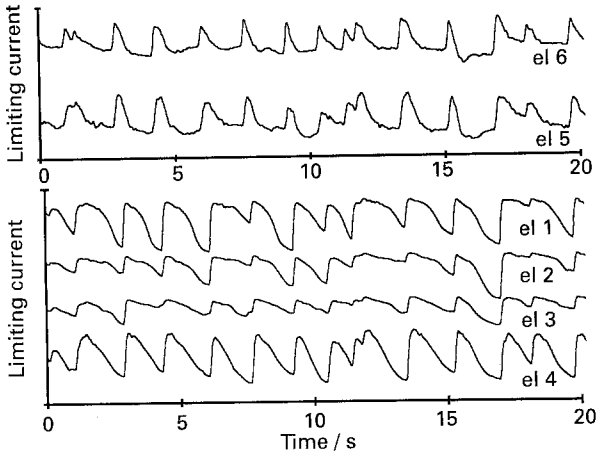

Fig. 4. Traces of instantaneous liquid–solid mass transfer coefficient in pulsing flow (limiting current mA cm^{-2}), obtained simultaneously with small embedded circular electrodes (5, 6) and spherical electrodes (1, 2, 3, 4). Mean mass fluxes $L = 6.019\,kg\,m^{-2}\,s^{-1}$ and $G = 0.274\,kg\,m^{-2}\,s^{-1}$.

sage of the liquid-rich region of a pulse. A gradual decrease of the limiting current is associated with the gas-rich region. The greater fluctuations displayed in traces from electrodes 4 and 1 are attributed to relatively larger local voidage. For this presentation, traces in Fig. 4 have been smoothed by applying a low pass filter. This smoothing procedure slightly affects the traces from the microelectrodes, eliminating only high frequencies, but leaving unaltered all their essential features; i.e. pulse shape and characteristic frequency. It must be added here that values of standard deviation from these and other time series, show that the intensity of fluctuations is affected more by changes of mean liquid flow rate than by similar changes of gas flow.

It is interesting that the passage of a pulse is clearly detected by all the cathodes, spherical as well as small circular electrodes. It is worth noticing that the microelectrode facing the flow (5) has an output very similar to that of the microelectrode facing the bottom of the bed (6). Small differences among the signals are attributed to local non-uniformities of porosity or flow. The similarity of all these simultaneous traces is clear evidence that the pulse disturbances uniformly

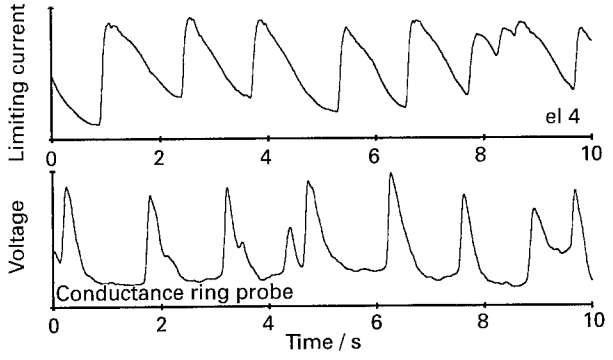

Fig. 5. Comparison of traces representing local mass transfer rate to a particle (electrode 4) and cross-sectional average holdup (voltage V) obtained by the ring probe, under pulsing flow conditions ($L = 6.019\,kg\,m^{-2}\,s^{-1}$ and $G = 0.328\,kg\,m^{-2}\,s^{-1}$).

penetrate even the smallest three-dimensional packing constrictions, possibly resulting in periodic fluid renewal therein. The power spectral density functions from all these simultaneous traces display a single peak indicative of the dominant pulse frequency. Since the electrodes are in various radial locations, these results suggest that the pulses cover the entire cross section of the packed bed.

Comparison of pulsing flow characteristics that manifest themselves in a small, as well as in a large, length scale can be made in Fig. 5, where traces from two different methods are displayed. The trace of local mass transfer at the top is taken by the electrodiffusion technique (spherical electrode 4), while the one at the bottom represents cross-sectionally averaged instantaneous holdup obtained with a conductance technique described by Tsochatzidis and Karabelas [20]. These traces are from the same run, but not simultaneous. It is clear that the pulse frequency is reflected equally well in both traces. The pulse front is associated with a steep increase of both holdup and mass transfer. However, while the cross-sectional average holdup tends to drop rather sharply after the passage of the liquid-rich portion of the pulse, the mass transfer rate is maintained longer at a relatively high level. It is also observed that the peak values of mass transfer rate tend to remain relatively constant, for a set of flow conditions, while this may not be the case for the corresponding maximum holdup. Similarly observations are reported by Chou *et al.* [8] who compare mass transfer and pressure signals in pulsing flow.

3.3. *Radial distribution in pulsing flow*

There is considerable uncertainty in the literature concerning the possibly uneven radial distribution of mass transfer rates. Using the electrochemical technique, Chou *et al.* [8] report that in the pulsing flow regime the time averaged quantity ϕSh is essentially independent of either axial or radial location. Furthermore, arguing that it is unlikely that exactly the same *partial* wetting exists simultaneously at different locations in the bed, they conclude that uniform and complete wetting of particles exists. Gabitto and Lemcoff [9], using the same technique in a relatively small diameter bed (7 cm i.d.) packed with beads 4.8 mm in diameter, present data taken in pulsing flow. The mass transfer coefficient at the centre and near the bed wall appear to be of similar magnitude, while those in the middle are smaller. Lemay *et al.* [21] employ the dissolution technique to determine mass transfer to a layer of active spheres placed at three radial positions in the bed. Their packing is 6 mm in diameter spheres and the bed i.d. 7.6 cm. Their results suggest that the mass transfer coefficient is not very sensitive to radial position, although data obtained from the central region of the bed are higher than those from other positions.

Data from this study on the radial dependence of time-averaged mass flux, obtained with four active

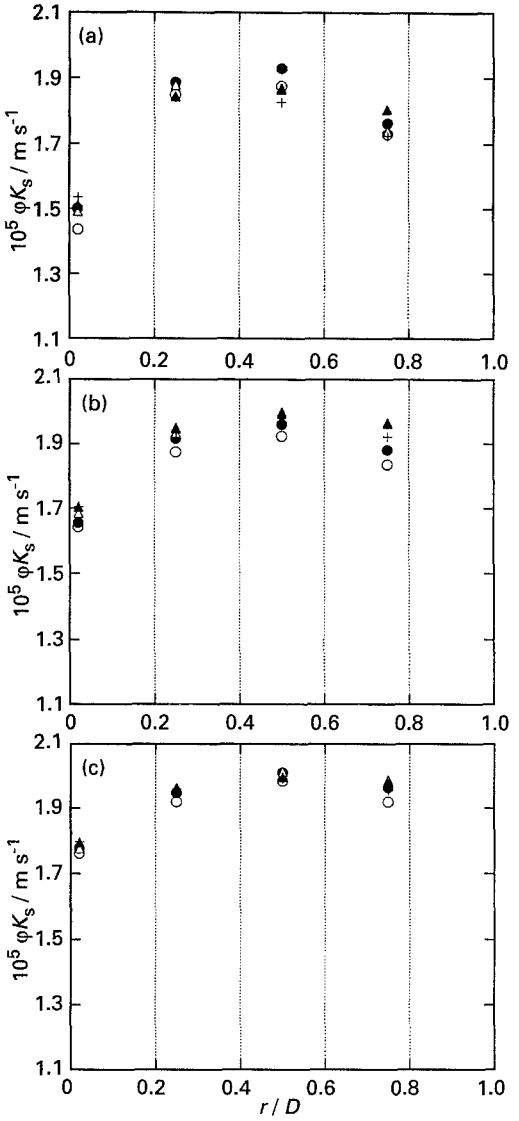

Fig. 6. Radial variation of time averaged mass transfer coefficient to a spherical particle under pulsing flow conditions. (a) For $L = 6.019\,\mathrm{kg\,m^{-2}\,s^{-1}}$, G: (○) 0.220, (●) 0.246, (△) 0.274, (▲) 0.328 and (+) $0.358\,\mathrm{kg\,m^{-2}\,s^{-1}}$. (b) For $L = 7.589\,\mathrm{kg\,m^{-2}\,s^{-1}}$, G: (○) 0.121, (●) 0.146, (△) 0.198, (▲) 0.252 and (+) $0.278\,\mathrm{kg\,m^{-2}\,s^{-1}}$. (c) For $L = 9.159\,\mathrm{kg\,m^{-2}\,s^{-1}}$, G: (○) 0.097, (●) 0.148, (△) 0.201, (▲) 0.255 and (+) $0.283\,\mathrm{kg\,m^{-2}\,s^{-1}}$.

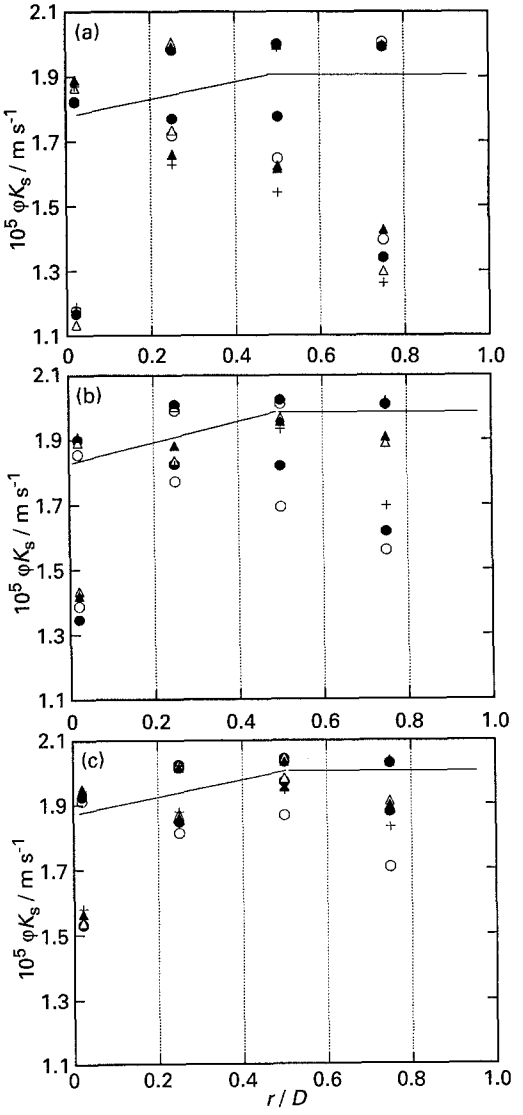

Fig. 7. Radial variation of mass transfer rates in pulsing flow. Local time averaged *peak* values (liquid-rich part of the pulses) above the line; local time averaged *minimal* values (gas-rich part of the pulses) below the line. (a) For $L = 6.019\,\mathrm{kg\,m^{-2}\,s^{-1}}$, G: (○) 0.220, (●) 0.246, (△) 0.274, (▲) 0.328 and (+) $0.358\,\mathrm{kg\,m^{-2}\,s^{-1}}$. (b) For $L = 7.589\,\mathrm{kg\,m^{-2}\,s^{-1}}$, G: (○) 0.121, (●) 0.146, (△) 0.198, (▲) 0.252 and (+) $0.278\,\mathrm{kg\,m^{-2}\,s^{-1}}$. (c) For $L = 9.159\,\mathrm{kg\,m^{-2}\,s^{-1}}$, G: (○) 0.097, (●) 0.148, (△) 0.201, (▲) 0.255 and (+) $0.283\,\mathrm{kg\,m^{-2}\,s^{-1}}$.

spherical electrodes, are presented in Fig. 6. $r/D = 0.5$ corresponds to the bed centerline. Three sets of data are plotted in Fig. 6 for different gas flow rates while the liquid flow rate is held constant in each set. These data correspond to well developed pulsing flow, but not very far from the trickling-to-pulsing transition. Higher ϕK_s values are measured at the centre of the bed. Relatively lower values of the mass flux are measured near the wall of the cylindrical column, probably due to the increased porosity and the reduced local gas velocity. Small differences between values taken with electrodes 1 and 3, equidistant from the centre, are attributed to local porosity nonuniformities. These data give the impression of a parabolic distribution. Nevertheless, in general the differences in mass transfer rates throughout most of the bed cross section (excluding the region close to the column wall) are not very significant; i.e. less than 10%. Furthermore, by increasing the liquid flow rate the local mass fluxes tend to become more uniform.

For the flow rates examined in this work, the gas flow appears to have an insignificant influence on the mass transfer rate, in the pulsing regime. The same observation is reported in the very recent study by Sims *et al.* [22] who measured solid–liquid mass transfer to hollow pellets in a trickle bed, in about the same range of flow rates.

Useful information is obtained by plotting in Fig. 7 data for the radial variation of mass flux, separately for the liquid-rich and the gas-rich region of the pulses. Similar data are reported only by Rao and Drinkenburg [7] and only from the centre of a bed packed with cylinders. The lines in Fig. 7 simply separate the two sets of experimental points. Data of Fig. 7 are extracted in the following way. Using a computer

program the peak and trough values of each pulse are determined in traces like those of Fig. 4(b). By averaging the peak and the trough values the mass transfer rate is calculated in the liquid-rich and the gas-rich region, respectively. The standard deviation of the peak values is 1–3% of their respective mean values, while that of the trough values is 3–15%. The larger variation in the trough values may be explained by using the qualitative observations of the traces made in the previous section. Data of ϕK_s for the gas-rich region show much greater spread than those for the liquid-rich region. The latter are almost constant throughout the cross section irrespective of the flow rates. However, the general validity of this observation must be confirmed over a larger range of liquid flow rates than that examined here. Some deviations are measured next to the wall and are attributed to the larger local voidage. An increase of the liquid flow rate tends to reduce data scattering in the gas-rich part of the pulse. It appears also that electrode 1 is placed in a region of somewhat larger porosity compared to electrode 3.

4. Concluding remarks

Using the electrodiffusion method useful local mass transfer data were obtained in a trickle bed operating in the pulsing flow regime. Measurements with spherical electrodes (of diameter equal to the packing material) show that there is a relatively small radial variation of the time averaged mass transfer coefficient. Lower values of ϕK_s were obtained close to the bed wall, while throughout the rest of the bed these variations were not significant.

It is shown here that small circular electrodes, embedded into the surface of particles, offer the possibility of exploring the local transport phenomena on a very small length scale, representative of the pores of the bed. However, more measurements of such local mass fluxes and shear stresses are clearly needed.

By reviewing all the experimental evidence obtained so far, the following picture can be painted concerning pulsing flow. In the liquid-rich region complete and *radially uniform* wetting appears to take place, resulting in radially almost constant mass transfer rates. In the gas-rich region, considerably smaller mass transfer rates are measured. Local voidage nonuniformities are more evident in this part of the pulse. The time averaged mass transfer rates over a particle are mainly influenced by the high values associated with the liquid rich region.

Acknowledgements

The authors are grateful to the Commission of European Communities for financial support of this work under contract JOU2-CT92-0067. N. A. Tsochatzidis would also like to extend his gratitude to Bodossakis Foundation for a scholarship.

References

[1] M. Herskowitz and J. M. Smith, *AIChE J.* **29** (1983) 1.
[2] J. C. Charpentier, *Chem. Eng. J.* **11** (1976) 161.
[3] A. Gianetto, G. Baldi, V. Specchia and S. Sicardi, *AIChE J.* **24** (1978) 1087.
[4] H. Hofmann, *Int. Chem. Eng.* **17** (1977) 19.
[5] A. Gianetto and V. Specchia, *Chem. Eng. Sci.* **47** (1992) 3197.
[6] J. M. de Santos, T. R. Melli and L. E. Scriven, *Annu. Rev. Fluid Mech.* **23** (1991) 233.
[7] V. G. Rao and A. A. H. Drinkenburg, *AIChE J.* **31** (1985) 1059.
[8] T. S. Chou, F. L. Worley, Jr. and D. Luss, *Ind. Eng. Chem. Fundam.* **18** (1979) 279.
[9] J. F. Gabitto and N. O. Lemcoff, *Chem. Eng. J.* **35** (1987) 69.
[10] M. A. Latifi, S. Rode, N. Midoux and A. Storck, *Chem. Eng. Sci.* **47** (1992) 1955.
[11] S. L. Gordon, J. S. Newman and C. W. Tobias, *Ber. Bunsenges. Phys. Chem.* **70** (1966) 414.
[12] J. R. Selman and C. W. Tobias, 'Advances in Chemical Engineering' Vol. 10, Academic Press, New York (1978) pp. 211–318.
[13] V. Specchia, G. Baldi and A. Gianetto, *Ind. Eng. Chem. Process Des. Dev.* **17** (1978) 362.
[14] T. Hirose, Y. Mori and Y. Sato, *J. Chem. Eng. Jpn.* **9** (1976) 220.
[15] K. R. Jolls and T. J. Hanratty, *AIChE J.* **15** (1969) 199.
[16] A. J. Karabelas, T. H. Wegner and T. J. Hanratty, *Chem. Eng. Sci.* **26** (1971) 1581.
[17] *Idem, ibid.* **28** (1973) 673.
[18] T. R. Melli, J. M. de Santos, W. B. Kolb and L. E. Scriven, *Ind. Eng. Chem. Res.* **29** (1990) 2367.
[19] P. G. Lutran, K. M. Ng and E. P. Delikat, *ibid.* **30** (1991) 1270.
[20] N. A. Tsochatzidis and A. J. Karabelas, *in* Proc. 2nd world conf. on 'experimental heat transfer, fluid mechanics and thermodynamics' (edited by J. F. Keffer, R. K. Shah, E. N. Ganic) Elsevier, Amsterdam (1991) pp. 1515–1522.
[21] Y. Lemay, G. Pineault and J. A. Ruether, *Ind. Eng. Chem. Process Des. Dev.* **14** (1975) 280.
[22] W. B. Sims, F. G. Schulz and D. Luss, *Ind. Eng. Chem. Res.* **32** (1993) 1895.